An Intelligent Fault Diagnosis Method based on STFT and Convolutional Neural Network for Bearings Under Variable Working Conditions

Dawei Zhong[1], Wei Guo[1,2], Da He[1]
1. School of Mechanical and Electronical Engineering,
University of Electronic Science and Technology of China (UESTC), Chengdu, China
2. Institute of Electronic and Information Engineering of UESTC in Guangdong, Guangdong, China
E-mail: gwuestc2013@163.com

***Abstract*—The faults on rolling bearings, one of key components in various rotating machinery, are usually main source of many failures in these devices. It leads to many attentions by engineers and scholars who expect to accurately diagnosis their faults as early as possible to prevent chain accident. Many diagnosis methods are reported to process the cases under the constant speed or load, while the reality on this is often harsh and variable, which limits the accuracy of bearing diagnosis. To address this problem, an intelligent fault diagnosis model is put forward by combining the short-time Fourier transform (STFT) and the convolutional neural network (CNN), the former of which is used to transform the vibration signal in time domain to time-frequency domain and further forms inputs of the latter. Experimental data accumulated from six bearings under two conditions are applied to verify the effectiveness and accuracy of the diagnosis model. The damages on the bearing outer or inner race are actually generated during the accelerated life time tests and are still at the early stage, which are quite different from artificial damages and make the accurate diagnosis harder. Analyses and comparisons of the experiment results demonstrate the feasibility and higher diagnosis accuracy of the intelligent diagnosis model.**

Keywords- convolution neural network; fault diagnosis; short-time Fourier transform; variable working condition; rolling bearing.

I. INTRODUCTION

As an important component in manufacturing industry, bearings are widely used in various mechanical equipment, especially in the area of motor [1-3], urban rail train [4], gearbox [5-6] and so on. With the increasingly high-quality requirements for various types of mechanical equipment, condition monitoring for bearings plays an important role for their safety and reliability operation. It is reported that damages are easily existed in bearings under harsh working environment and further affect their service life [7]. Furthermore, their damage may cause their failure and chain reactions on adjacent machine components and the whole rotating machinery. Therefore, it is critical to put forward an effective and applicable method to identify bearing fault state so that it not only reduces the probability of accidents but also saves maintenance costs.

At present, condition monitoring and fault diagnosis of bearing is still a hot topic. Vibration monitoring is proven to be a useful way to analyze and identify bearing failure. The key of the vibration-data-driven fault diagnosis is to identify the cyclo-stationary property of impacts and/or the corresponding characteristics in time and/or frequency domains. For real applications, the difficulty of the bearing diagnosis is that the bearing signal is contaminated by strong noise and other vibration signals, and the theoretical characteristic defect frequencies are different from the real one due to variation of rotating speed and operations, so that it is still a challenge task to provide accurate fault diagnosis for real bearings.

Recent development on advanced signal processing methods and artificial intelligence provide possible solutions on bearing fault diagnosis. Qin [8] considered the problem that approximately periodic impulses in raw signals are usually contaminated by background noise and other strong vibrations and then proposed a hybrid feature extraction method by integrating an iterative thresholding shrinkage algorithm and the sparse representation so that repetitive impulses in vibrations are extracted. Li *et al*. [9] used the correlation analysis to implement the independence-oriented variational mode decomposition and adaptively extracted complex health condition features for the diagnosis of wheel set bearings. Ben Ali *et al*. [10] selected empirical mode decomposition energy entropy as the health index and inputs of an artificial neural network to automatically classify bearing faults. Wang *et al*. [11] used the binary wavelet packet transform to generate some waveform features and then used the manifold method to extract key features for fault classification. Zhang *et al*. [12] applied some wide kernels in the first convolutional layer of the convolutional neural network, which come true the feature extraction and high-frequency noise suppression. Li *et al.* [13] proposed an adaptive multi-scale morphological filter to preprocess raw signals and then the modified hierarchical permutation entropy of the filtered signal is used to classify health states of planetary gearboxes.

Since 2006, the deep learning attracts more attentions and is widely used in image processing, speech recognition and machine translation [14], and is also applied to the intelligent diagnosis of bearings. Wang *et al.* [15] provided a possible solution on the bottleneck of layer optimization of the

978-1-7281-0860-5/19/$31.00 ©2019 IEEE

convolutional neural network (CNN) and then applied to the fault recognition for rotating machines by fusing multi-sensor data. Feng *et al.* [16] proposed a deep normalized convolutional neural network to solve the problem caused by the imbalanced distribution of bearing conditions and then used the neuron activation maximization algorithm to illustrate the working principle of kernels in convolutional layers. Jia *et al.* [17] put forward the normalized sparse autoencoder, a network containing local connections, so that the network obtains some learned features with shift variant characteristics and overcomes the problem of misclassification. Han *et al*. [18] integrated the CNN with the spatiotemporal pattern network and then applied such a hybrid network to diagnosis unseen operation conditions and evaluate the extents of bearing damages. Ding *et al*. [19] firstly proposed to use the wavelet packet transformation to convert the vibration signals into soma 2D images and then combined with the CNN to improve the recognition accuracy of bearing states. Hoang and Kang [20] gave a review on three popular deep learning algorithms, i.e. the autoencoder, the restricted Boltzmann machine, and the CNN along with their applications to bearing fault diagnosis.

Although there are many publications on bearing fault diagnosis, most of them focus on the improvement of complicated structure and diagnosis accuracy, in which the analyzed bearing data are usually obtained under constant working conditions. In this paper, an intelligent fault diagnosis method is designed based on the short-time Fourier transform and the deep convolutional neural network, which is applied to identify the states of bearings under different conditions (rotating speeds, load torques and radial forces). The difficulty of this task lies in quite difference of vibrations from theoretical those and differences of vibrations among different conditions for the same bearing fault.

The remaining of this paper is organized as follows. Section II briefly introduces theoretical foundation on STFT and CNN. Section III shows the procedure and settings for the intelligent fault diagnosis method based on STFT and CNN in this paper. Section IV introduces the experimental data and then applied the diagnosis method to these data. After that, the critical parameter setting and multiple calculation results are analyzed and compared to verify the effectiveness of this diagnosis method. Finally, conclusions are drawn in Section V.

II. Brief Introduction on CNN

The convolutional neural network (CNN) is a multi-layer neural network, including some convolution layers, pooling layers, activation layers and fully-connected layers. The structure and learning algorithm of the fully-connected layer are the same as those of the normal feedforward neural network. The advantage of CNN lies in the structure and operation of convolution layer and pooling layer. CNN is a popular deep learning model at present. By convolution and activation, input features can be extracted. The pooling layer conducts the down-sampling so that the network can extract more complex features from larger-scale inputs. After multi-layer convolution and pooling, the features from data are directly used for classification. As a simple deep learning model, the CNN plays a significant role in feature extraction. The illustration of the CNN structure is shown in Figure 1.

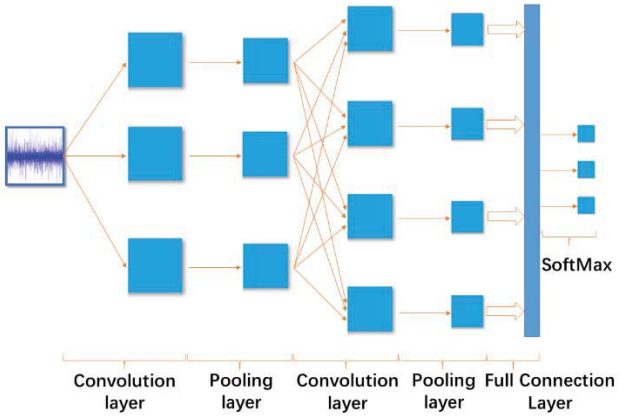

Figure 1. A convolution neural network.

A convolution layer contains several learnable convolution kernels, each of which has learnable weights and biases. In the convolution layer, the input convolutes with the kernel, and the result is entered into the activation function. After the operation in the activation function, the convolution layer generates the outputs. Assuming that x_i^{l-1} is the input of the l-th layer, the convolution result of this layer can be expressed as:

$$x_j^l = s_f\left(\sum_{i \in M_j} x_i^{l-1} * k_j^l + b_j^l\right) \tag{1}$$

where *, s_f, b_j^l, k_j^l and M_j are the convolution operation, the activation function, the bias, the convolution kernel in l-th layer and a collection of input images, respectively [20].

III. Bearing Fault Diagnosis Based on STFT and CNN

Based on the STFT and CNN, an intelligent fault diagnosis method is proposed for bearings under variable working conditions. First, raw vibration signals are processed by the STFT individually, and the corresponding results form inputs of the CNN. Some samples are selected to train the CNN model. Once the learning object is satisfied, the remaining samples are used as testing samples to show the generalization ability of the trained model; meanwhile, the fault type of the tested bearing can be determined. The measurement index is the popular diagnosis accuracy, i.e. the ratio of the correctly identified sample number to the total testing sample number.

The description on the designed CNN model in this paper is shown in Figure 2. This CNN model has of two convolution layers, two pooling layers and two fully connected layers. The specification on parameters of the CNN is shown in Table I. First, the result after applying the STFT to raw vibration data is a small image with 64×64 pixels. For the first convolution operation, 64 kernels of 3×3 size are chosen to convolute, and the results are then inputted into the activation function. After that, the result of operation enters the pooling layer. Here, the type of the pooling type is selected as the Max pooling, where the size is set to 3×3 and the step length is 2×2. The output of the pooling is 64 feature maps and the size are 64×64. In the second convolution operation, 16 kernels of 3×3 size are used to convolute, and the results of convolution are also inputted into the activation function and processed by the pooling layer again. The type and size of this pooling is the same as the first pooling layer, but the step length is set to 1×1. The pooling result is

reduced to 16 feature maps and the size of each map is 32×32. Finally, the SoftMax function is used to conduct the classification of health states in the full connection layer. In the next section, experimental data of bearings under different working conditions are applied to train this model.

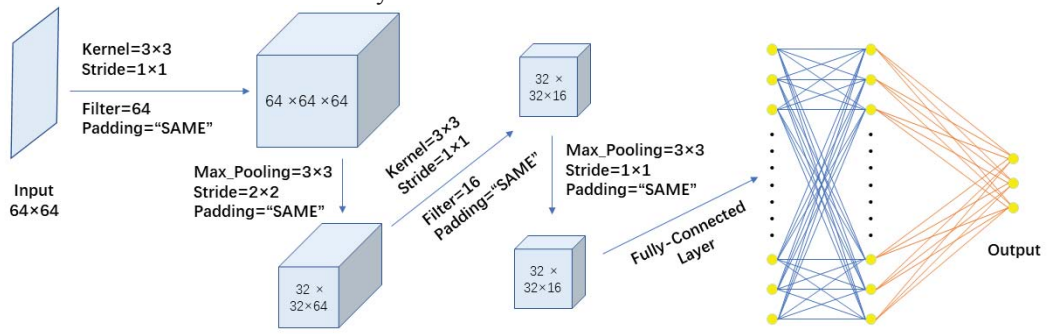

Figure 2. The proposed CNN model for bearing fault diagnosis.

TABLE I. MAIN PARAMETERS OF THE CNN MODEL

Layer	Settings for CNN	
Convolution Layer 1	The size of kernel	3×3
	The number of kernels	64
	The number of channels	1
	Stride length	1×1
Pooling Layer 1	The way of pooling	Max
	The size of pooling	3×3
	Stride length	2×2
Convolution Layer 2	The size of kernel	3×3
	The number of kernels	16
	The number of channels	64
	Stride length	1×1
Pooling Layer 2	The way of pooling	Max
	The size of pooling	3×3
	Stride length	1×1
Full Connection Layer	The way of classification	SoftMax
	The number of full Connections	2

IV. EXPERIMENTS AND ANALYSES

In this section, experimental data from the accelerated life time tests are collected and then used to verify the effectiveness of the proposed intelligent fault diagnosis method. After that, the parameter settings and multiple calculation results are compared and analyzed to demonstrate the accuracy of the diagnosis.

A. Specification on Experiments

The experiments were conducted by Lessmeier *et al*. from Paderborn University [21]. They completed two types of damages on the bearing components, i.e. artificial and real damages. In this paper, the experimental data involving real damages are used.

The bearing (type 6203) in the housing in Figure 3 was tested in the accelerated life time test (Figure 3). To accelerate the appearance of real damages on the bearings, a higher radial force and load torques were applied on the bearings. The sampling frequency is 64kHz.

After being marked, some experimental data sets are chosen for verification and their descriptions are shown in Table II. The applied sets are mainly from healthy bearings and faulty bearings with outer and inner race defects. For each bearing, two working conditions are considered, including 1) condition C1, i.e. the rotating speed of 900 rpm with a load torque of 0.7 Nm and a radial force 1000 N on the bearing; 2) condition C2, i.e. the rotating speed of 1500 rpm with a load torque of 0.1 Nm and a radial force 1000 N on the bearing.

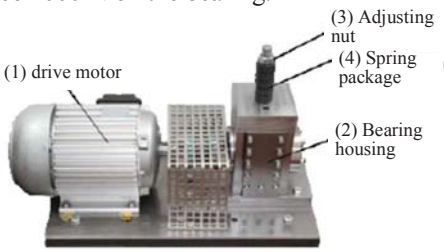

Figure 3. Apparatus for accelerated life time test [21]: (1) a drive motorr; (2) a housing;(3) adjusting nut; and (4) spring package.

TABLE II. DESCRIPTIONS ON EXPERIMENTAL DATA OF BEARINGS

Code	Damage mode	State	Arrangement of damage	Extent of damage	Condition
K003	\	Health	\	\	C1, C2
K006					C1, C2
KA15	Plastic deform	OR defect	Single damage	1	C1, C2
KA30			Repetitive damage	1	C1, C2
KI18	Fatigue: pitting	IR defect	Single damage	2	C1, C2
KI21				1	C1, C2

Notes: OR - Outer race; IR - Innter race;
C1 - the rotating speed of 900 rpm with a load torque of 0.7 Nm and a radial force 1000N on the bearing;
C2 - the rotating speed of 1500 rpm with a load torque of 0.1 Nm and a radial force 1000N on the bearing.

B. Vibration Signals and Their STFT Results

Some vibration signals for data sets in Table II under two working conditions are shown in Figures 4, 6 and 8. The settings of STFT are shown in Table III and some results after applying to STFT are shown in Figures 5, 7, and 9.

As shown in Figures 4 and 6, the amplitudes of signals from a healthy bearing are much larger than those from a bearing from the OR defect. Although signals in Figure 6 are marked with the same defect, their amplitudes and periods are quite different, which are from real damages and make the accurate diagnosis

difficult. Similar observations are also found in Figure 8.

It is noted that all experimental data are 4 seconds of signals, for example signals in Figure 4. To show the impulses caused by faulty bearing components clearly, the signals in 1 of 4 seconds are shown in Figures 6 and 8.

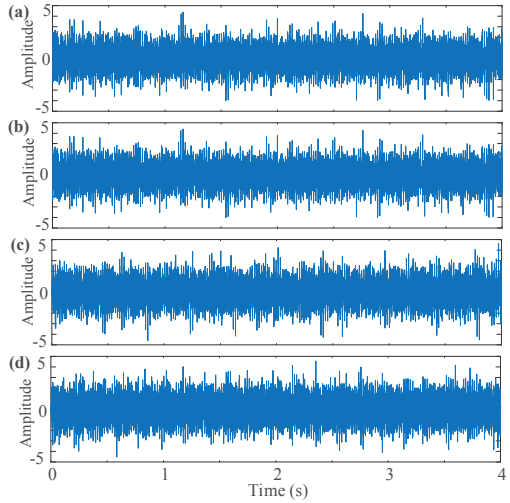

Figure 4. Vibration signals from healthy bearings under two conditions: (a) C1 in K003, (b) C2 in K003, (c) C1 in K006, and (d) C2 in K006.

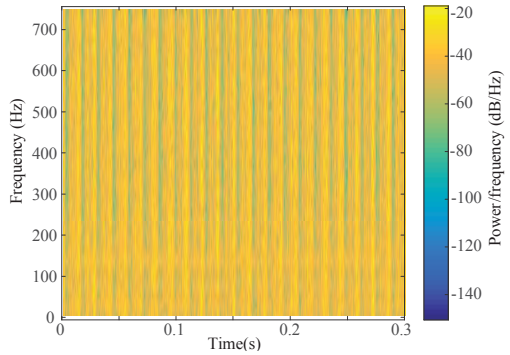

Figure 5. Part of STFT result of data K003 under C1 from a healthy bearing.

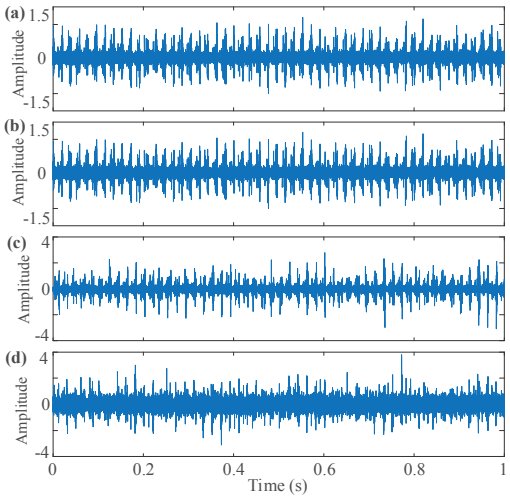

Figure 6. Vibration signals from bearings with outer race defect under two conditions: (a) C1 in KA15, (b) C2 in KA15, (c) C1 in KA30, and (d) C2 in KA30.

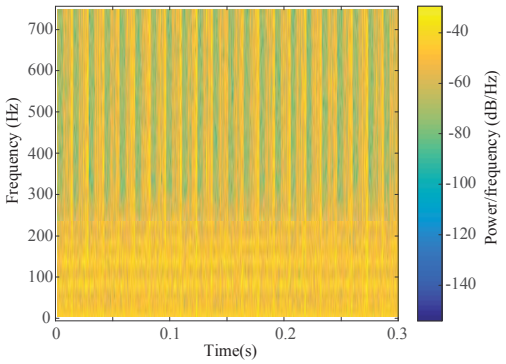

Figure 7. Part of STFT result data KA15 under C1 from a bearing with an outer race defect.

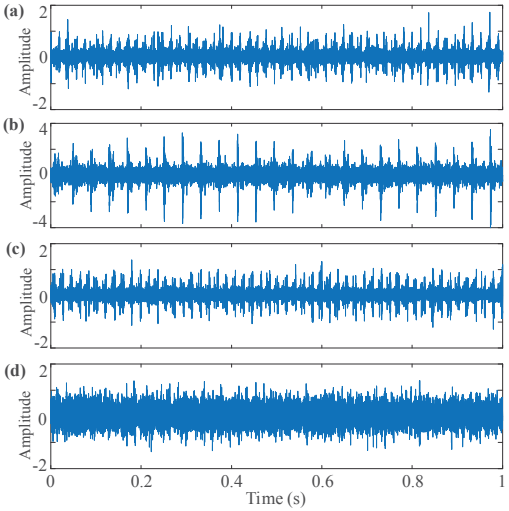

Figure 8. Vibration signals from bearing with inner race defect under two conditions: (a) C1 in KI18, (b) C2 in KI18, (c) C1 in KI21, and (d) C2 in KI21.

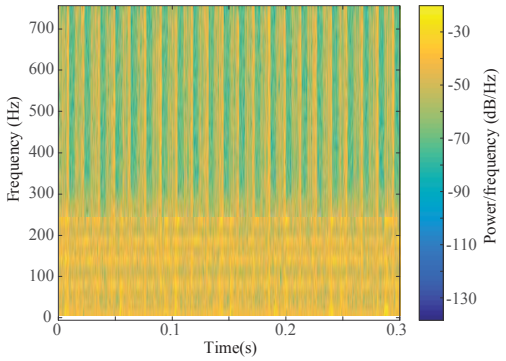

Figure 9. STFT result of part of data KI18 and conditon C1 from a bearing with an inner race defect.

TABLE III. SETTINGS FOR STFT

Window function	Number of segments	$N_{overlap}$	N_{fft}	f_s
Hamming	128	120	120	1500

The parameters in the table are: $N_{overlap}$ is the number of overlapped samples, N_{fft} is the number setting for fast Fourier transform, and f_s is the sampling frequency.

To train the CNN and test its generalization ability, 240

samples are generated based on the experimental data listed in Table II. For each bearing code, there are 20 data sets after individually collecting data from the same bearing and condition 20 times, and thus there are 40 data sets for two conditions of one bearing code. 240 data sets are obtained from six bearing codes. Considering that the first 0.3 second in the STFT results shown in Figures 5, 7 or 9 is enough to represent the characteristics in time-frequency domain of bearings, the small part of signals is used as one sample. After applying to the STFT, 240 samples are available for the CNN, in which 121 samples are randomly selected from 240 samples for training and the remaining 119 samples are used for testing. Such random selection will lead to different proportion among three kinds of samples, and its intent is to test the generalization ability of the proposed CNN model.

C. *Diagnosis Results and Analyses*

The training samples were inputted into the CNN. Since the learning rate is critical for weight updating in the CNN. If the learning rate is a very small value, the updating speed of parameters in the model is slow; if the learning rate is too large, the optimal solution may be lost. Therefore, an appropriate value for this parameter is needed for accurate diagnosis of the analyzed bearings. During the training stage, four values, i.e. 0.01, 0.001, 0.0001, 0.00001, are set. The corresponding losses and accuracies for each learning rate are calculated individually and the results for 500 iterations are shown in Figures 10 and 11, respectively.

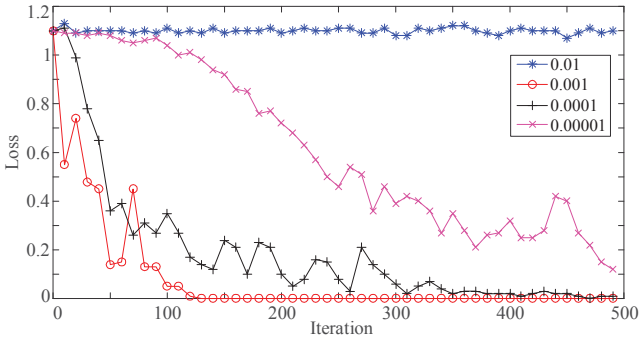

Figure 10. The loss in the training process when individually setting four learning rages of 0.01, 0.001, 0.0001 and 0.00001.

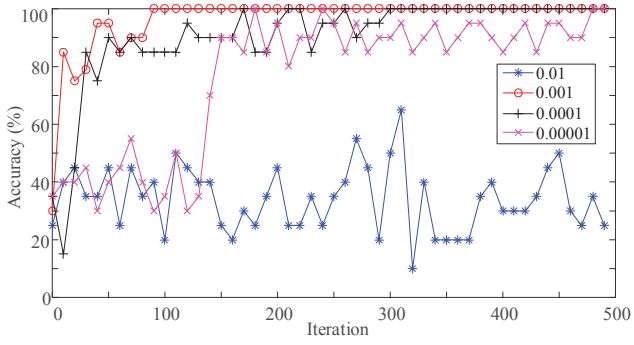

Figure 11. The diagnosis accuracy in the training process when individually setting four learning rates of 0.01, 0.001, 0.0001 and 0.00001.

The comparisons on the loss and accuracy among four learning rates demonstrate that a larger learning rate leads to low learning ability and fault type cannot be identified correctly, while the other three learning rates provide higher diagnosis accuracies at the end of 500 iterations. Further comparisons among these three settings, the results for the learning rate of 0.001 are better than those for the learning rate of a smaller value 0.0001. The former has the advantage of faster convergence and fewer iteration number. The results corresponding to the learning rate of a very small value, i.e. 0.00001, shows an obvious fluctuation trend though it finally reaches a lower loss and a higher accuracy. It indicates that a very small learning rate is unnecessary and then not recommended.

After selecting the learning rate of 0.001 and training the CNN, 119 samples are applied to the trained CNN model and the confusion matrix for the testing are shown in Figure 12.

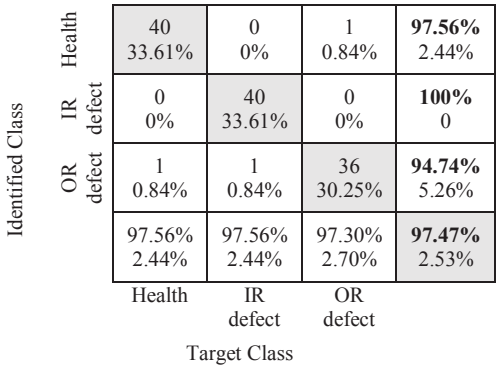

Figure 12. Validation data confusion matrix for one of calculations.

For the first column of the matrix, it indicates that there are 41 health samples, 40 of which are identified as 'health' and the diagnosis accuracy is 97.56% (40/41); 1 of which are wrongly identified as the outer race defect and the misdiagnosis rate is 2.44% (1/41). For the second column, there are also 41 samples from the bearing with an inner race defect, 40 of them are identified as 'IR defect' and the accuracy is then 97.56% (40/41), and 1 of them are wrongly classified as 'OR defect' and the misdiagnosis is also 2.44%. According to the third column, 36 of 37 samples from the bearing with an outer race defect are correctly identified and the diagnosis accuracy is 97.30% (36/37) and the misdiagnosis rate is 2.70% (1/37). The final diagnosis accuracy is (40+40+36)/(41+41+37) = 116/119, i.e. 97.47%, and then the misdiagnosis rate is 2.53%.

The first row in this matrix indicates that the trained CNN model labels 41 samples as 'health', while only 40 samples are healthy, and thus its accuracy is 97.56% (40/41). Similarly, 36 of 38 samples identified as OR defect are correct diagnosis and its accuracy is 94.74% (36/38), in which two samples are wrongly classified as 'health' and 'IR defect'.

The first three diagonal elements show correct diagnoses for three kinds of experimental data, i.e. 40 health samples, 40 IR detect samples, and 36 OR defect samples in the total 119 testing samples are correct diagnosis, and the corresponding accuracies are 33.61% (40/119), 33.61% (40/119), and 30.25% (36/119), respectively. For one sample rarely identified, its rate to the total testing samples is 0.84% (1/119). The above results indicate that most of testing samples are correctly identified by the trained CNN.

Further investigating the influence by the selection of training and testing samples, another nine random sample selections are conducted, and the corresponding classification accuracies are shown in Table IV. The average accuracy for bearing diagnosis is 97.48%, which demonstrates good

performance of the CNN model on bearing fault diagnosis.

TABLE IV. CLASSIFICATION ACCURACIES OF THE CNN FOR TEN CALCULATIONS

No.	Health	OR defect	IR defect	Classification accuracy
1	40/41	36/37	40/41	116/119 (97.47%)
2	44/44	35/36	37/39	116/119(97.47%)
3	39/39	39/40	40/40	118/119(99.16%)
4	39/39	37/39	39/41	115/119(96.64%)
5	39/40	40/41	36/38	115/119(96.64%)
6	40/40	37/39	39/40	116/119(97.48%)
7	40/42	39/40	36/37	115/119(96.64%)
8	38/38	37/38	41/43	116/119(97.48%)
9	40/41	39/40	37/38	116/119(97.48%)
10	36/36	41/43	40/40	117/119(98.32%)

V. CONCLUSIONS

Since it is very common that working conditions of bearings are variable, this paper put forward an intelligent fault diagnosis method by combining the STFT and the CNN, and then apply it to the experimental data from various bearings with different conditions. The characteristics in time-frequency domain obtained by the STFT, instead of raw vibration signals, are used as inputs of the CNN. The results of diagnoses and comparisons indicate that, although vibration signals are markedly different from theoretical or simulated ones and working conditions are not constant, the diagnosis accuracy is still higher, and its average value reaches to 97.48%. Two comparisons also give different indications on the performance of the CNN model. The first comparison of four learning rates further verifies the importance of setting learning rate, which is worthy to study its optimization. Another comparison on random selection of training and testing samples shows a minor change on diagnosis accuracy and indicate few changes on accurate bearing diagnosis for random sample selection. In our future work, optimizations on the parameters and structure of the CNN will be studied.

ACKNOWLEDGMENTS

The work described in this paper is fully supported by the Natural Science Foundation of Guangdong Province under Grant 2017A030313278, the Fundamental Research Funds for the Central Universities (No. ZYGX2018J045), and the National Natural Science Foundation of China (Nos. 71771038, 51537010 and 61833002).

REFERENCES

[1] A. Glowacz, "Fault diagnosis of single-phase induction motor based on acoustic signals," Mechanical Systems and Signal Processing, vol. 117, pp. 65-80, 2019.

[2] M.E.A. Khodja, A.F. Aimer, A.H. Boudinar, N. Benouzza and A. Bendiabdellah, "Bearing fault diagnosis of a PWM inverter Fed-Induction motor using an improved short time Fourier transform," Journal of Electrical Engineering & Technology, Singapore, vol. 14. pp.1201-1210, May 2019.

[3] A. Glowacz, "Acoustic based fault diagnosis of three-phase induction motor, " Applied Acoustics, vol.137, pp. 82-89, 2018.

[4] G.Q. Cai, C. Yang, Y. Pan, J.J. Lv, "EMD and GNN-AdaBoost fault diagnosis for urban rail train rolling bearings," Discrete and Continuous Dynamical Systems, vol. 12, pp. 1471-1487, 2019.

[5] V. Inturi, G.R. Sabareesh, K. Supradeepan, and P.K. Penumakala, "Integrated condition monitoring scheme for bearing fault diagnosis of a wind turbine gearbox," Journal of Vibration and Control, vol. 25, pp. 1852-1865, 2019.

[6] G.Q. Jiang, H.B. He, J. Yan, and P. Xie, "Multiscale convolutional neural networks for fault diagnosis of wind turbine gearbox," IEEE Transactions on Industrial Electronics, vol. 66, no. 4, pp. 3196-3207, 2019.

[7] L.L. Cui, X. Wang, Y.G. Xu, H. Jiang, and J.P. Zhou, "A novel switching unscented Kalman filter method for remaining useful life prediction of rolling bearing," Measurement, vol. 135, pp. 678-684, 2019.

[8] Y. Qin, "A new family of model-based impulsive wavelets and their sparse representation for rolling bearing fault diagnosis," IEEE Transactions on Industrial Electronics, vol. 65, no. 3, pp. 2716-2726, 2018.

[9] Z.P. Li, J.L. Chen, Y.Y. Zi, and J. Pan, "Independence-oriented VMD to identify fault feature for wheel set bearing fault diagnosis of high speed locomotive," Mechanical Systems and Signal Processing, vol. 85, pp. 512-529, 2017.

[10] J. Ben Ali, N. Fnaiech, L. Saidi, B. Chebel-Morello, and F. Fnaiech, "Application of empirical mode decomposition and artificial neural network for automatic bearing fault diagnosis based on vibration signals," Applied Acoustics, vol. 89, pp. 16-27, 2015.

[11] Y. Wang, G.H. Xu, L. Liang, and K.S. Jiang, "Detection of weak transient signals based on wavelet packet transform and manifold learning for rolling element bearing fault diagnosis," Mechanical Systems and Signal Processing, London, vol. 54-55, pp. 259-276, 2015.

[12] W. Zhang, G.L. Peng, C.H. Li, Y.H. Chen, and Z.J. Zhang, "A new deep learning model for fault diagnosis with good anti-noise and domain adaptation ability on raw vibration signals," Sensors, vol. 17, no. 2, 425(21 pages), 2017.

[13] Y.B. Li, G.Y. Li, Y.T. Yang, X.H. Liang, and M.Q. Xu, "A fault diagnosis scheme for planetary gearboxes using adaptive multi-scale morphology filter and modified hierarchical permutation entropy," Mechanical Systems and Signal Processing, vol. 105, pp. 319-337, 2018.

[14] R. Zhao, R.Q. Yan, Z.H. Chen, K.Z. Mao, P. Wang and R.X. Gao, "Deep learning and its applications to machine health monitoring," Mechanical Systems and Signal Processing, vol. 115, pp. 213-237, 2019.

[15] H.Q. Wang, S. Li, L.Y. Song and L.L. Cui, "A novel convolutional neural network based fault recognition method via image fusion of multi-vibration-signals" Computers in Industry, vol.105, pp. 182-190, 2019.

[16] F. Jia, Y.G. Lei, N. Lu and S.B. Xing, "Deep normalized convolutional neural network for imbalanced fault classification of machinery and its understanding via visualization," Mechanical Systems and Signal Processing, vol.110, pp. 349-367, 2018.

[17] F. Jia, Y.G. Lei, L. Guo, J. Lin, and S.B. Xing, "A neural network constructed by deep learning technique and its application to intelligent fault diagnosis of machines," Neurocomputing, vol.272, pp. 619-628, 2018.

[18] T. Han, C. Liu, L.J. Wu, S. Sarkar, and D.X. Jiang, "An adaptive spatiotemporal feature learning approach for fault diagnosis in complex systems," Mechanical Systems and Signal Processing, vol.117, pp. 170-187, 2019.

[19] X.X. Ding, Q.B. He, "Energy-fluctuated multiscale feature learning with deep ConvNet for intelligent spindle bearing fault diagnosis," IEEE Transactions on Instrumentation and Measurement, vol. 99, pp. 1-10, 2017.

[20] D.T. Hoang and H.J. Kang, "A survey on deep learning based bearing fault diagnosis," Neurocomputing, vol.335, pp. 327-335, 2019.

[21] C. Lessmeier, J.K. Kimotho, D. Zimmer and W. Sextro, "Condition monitoring of bearing damage in electromechanical drive systems by using motor current signals of electric motors: a benchmark data set for data-driven classification," European conference of the prognostics and health management society, 2016.